Study on Microstructure and Mechanical Properties of IGBT Module Bonding Interface after Multiple Reflowing

Xiankun Zhang[1], Xiaofei Pan[1], Xiaodong Zhang[1], Yuancheng Liu[1], Bin Chen[1], Aoao Ren[1]
[1]China Resources Runan Chongqing Co., Ltd., Shapingba, Chongqing 4000000, China

Corresponding author: Xiaofei Pan, Xiaofei_Pan@anst.crmicro.com
Speaker: Xiankun Zhang, xiankun_zhang@crmicro.com

Abstract

In this paper, the growth and morphology of intermetallic compound(IMC) at Die /Solder A/DBC, Mo/Solder A /Die and Mo/Solder A/DBC interfaces under different reflow times were studied. The shear strength and fracture mode of bonding interfaces under different reflow times was also studied. The resulted show that the thickness of IMC increases with the increase of reflow times, and the increasing rate of IMC thickness decreases with the increase of reflow times. The shear strength of Mo/Solder A/Die interface first increases and then decreases with the increase of reflow times. With the increase of reflow times, the fracture mode of bonding interface changed from ductile fracture which occurred at Sn matrix to mixed fracture mode which occurred Sn matrix and IMC. The Mo/Solder A/DBC interface after primary reflow is a mixed fracture mode which occurred at Cu_6Sn_5 phase, $(Cu, Ni)_6Sn_5$ phase and Sn matrix, and brittle fracture is the main fracture mode. After secondary reflow, the bonding interface is changed to brittle fracture which occurred at Cu_6Sn_5 phase and $(Cu, Ni)_6Sn_5$ phase.

Keywords: Multiple reflow; Sn-Ag-Cu solder; IMC; shear strength.

1 Introduction

Over the past several decades, Pb-Sn systems have been the mainstay of the conventional solder process owing to their unique combination of material properties and low cost [1]. However, medical studies have shown that Pb is a heavy metal toxin that can damage the kidney, liver, blood and the central nervous system[2,3]. In recent years, the lead free solder alloy system is widely used for electronic applications as a replacement for Sn-Pb eutectic alloy, which widely used is Sn-Ag-Cu solder. Several issues in using lead free solder have been reported, such as excessive growth of IMC, microvoid formation at the interface between Cu substrate and solder[4-7], and known that the thickness and morphology of the IMC have a great impact on the thermal fatigue life, isothermal shear fatigue life, tensile strength and fracture toughness of solder joints, but the most studies focus on integrated circuit device. Therefore, it is necessary to investigate the IMC growth behavior and mechanical properties in power devices. In this paper, the growth and morphology of IMC at IGBT module bonding interfaces under different reflow times were studied. The shear strength and fracture mode of bonding interfaces under different reflow times was also studied.

2 Experimental Methods

In this paper, IGBT module was manufactured by multiple reflowing. Which schematic diagram like Fig.1. The Die /Solder A/DBC and Mo/Solder A /Die interface was manufactured by three times reflowing. The Mo/Solder A/DBC interfaces was manufactured by two times reflowing.

In order to observe the cross section of solder joints, the prepared samples were cut into proper size and mounted in epoxy and then subjected to manually grind down to 4000 grit on a sandpaper. Next, these samples were polished by using diamond paste, and subsequently etched with a solution of 3%HCl+97%CH3COOH. The interfacial structures of samples and morphologies of interfacial IMC grains were observed by scanning electron microscopy (SEM). An X-ray microanalysis using energy dispersive spectroscopy (EDS) allowed the SEM to qualitatively analyze the elements present in a selected area of backscattered electron image. The equivalent thickness of the IMC was measured using the SEM image of the metallographic cross-sections and the following image analysis procedure. To improve the statistical reliability of the IMC layer-thickness data, at least 15 SEM images covering numerous grains in the middle of the interface were analyzed for each sample.

 DOI:10.30420/566414026

In order to obtain the shear strength of the connection interface, the sample is tested with a thrust testing machine. The pushing speed is 200um/s. Finally, the average value is taken to obtain the shear strength of the soldering interface. The fracture morphology of the joint is observed and analyzed with SEM and optical microscope.

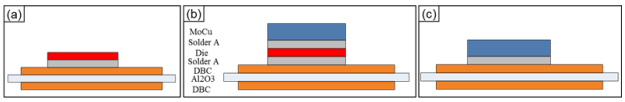

Fig.1. Variation curve of shear force and deformation of welded joint under different welding pressure

3 Results and discussion

3.1 Growth behavior and morphology analysis of IMC at soldering interface

Fig.2 showing the interfacial cross section SEM and IMC average thickness of Die/Solder A/DBC bonding interface under different reflow times. It is resulted that the planar-type Cu_6Sn_5 IMC formed at the soldering interface of Solder A/DBC after primary reflow. And the average thickness of Cu_6Sn_5 IMC layer in the Solder A/DBC interface is reference value which as ratio 1. After secondary reflow, the IMC layer is compact and the average thickness of IMC layer is 1.95 times. After triple reflow, the average thickness of IMC layer is 2.52 times.

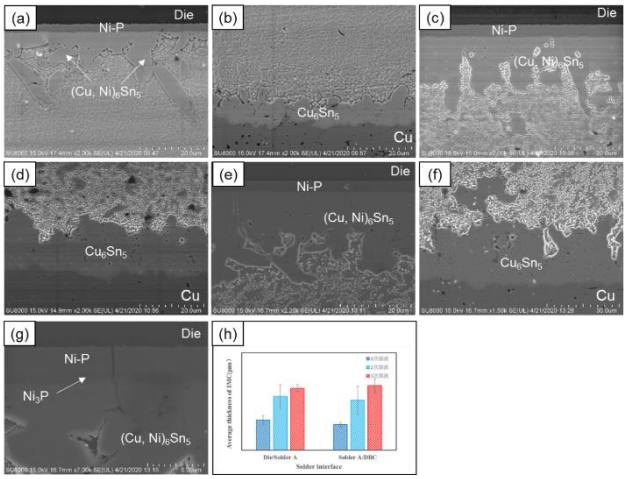

Fig.2. Interfacial Cross section SEM and IMC average thickness of Die/Solder A/DBC bonding interface under different reflow times. (a) (b) Primary reflow; (c) (d) Secondary reflow; (e) (f) (g) Triple reflow; (h) IMC average thickness after different reflow times.

After primary reflow at the Die/Solder A interface, scallop shaped and short rod shaped (Cu, $Ni)_6Sn_5$ intermetallic compounds were generated at the soldering interface, with an average thickness of 1.18. After secondary reflow, the scallop like and short rod like (Cu, $Ni)_6Sn_5$ phases disappear at the soldering interface, while the (Cu, $Ni)_6Sn_5$ phase grows into a planar shape with peaks and valleys, the average thickness of IMC layer is 2.1 times.

After triple reflow, the average thickness of (Cu, $Ni)_6Sn_5$ increased to 2.42 times, and cracks were observed on the Ni plated layer. This is because during the soldering process, the amorphous Ni-P+ will transform into crystalline Ni3P, which generating high shrinkage stress, resulting in cracks in the Ni plated layer and reducing the reliability of the connection interface.

Fig.3 showing the interfacial cross section SEM and IMC average thickness of Mo/Solder A/Die bonding interface under different reflow times. It is resulted that the planar-type (Ni, $Cu)_3Sn_4$ IMC formed at the soldering interface of Mo/Solder A and Solder A/Die solder joints after primary reflow, the average thickness of IMC layer is 2.77 times and 1.05 times, respectively. The IMC thickness of the Mo/Solder A interface is significantly greater than that of the Solder A/Die interface. This is because during the cooling process, the temperature of the Mo/Solder A interface is lower than that of the Solder A/Die interface. The presence of temperature gradient causes Ni atoms diffuser towards the Mo/Solder A interface, accelerating the growth of the (Ni, $Cu)_3Sn_4$ phase at the Mo/Solder A interface. Cracks were also observed at the interface between the Ni plating layer and MoCu alloy, which may be due to poor adhesion between the Ni plating layer and MoCu alloy, resulting in cracks propagating along the interface under thermal stress.

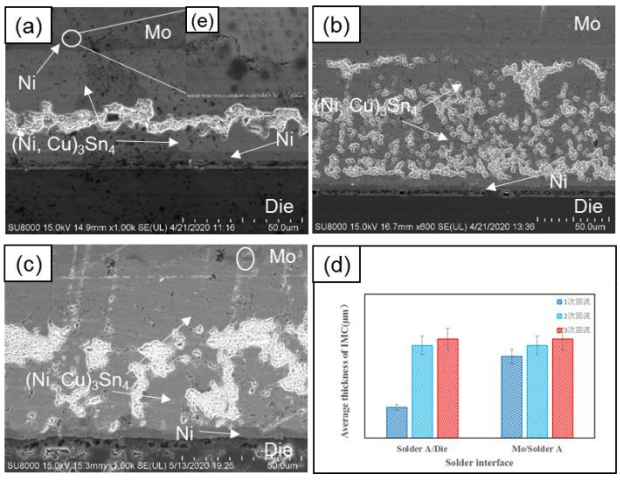

Fig.3. Cross section SEM and IMC average thickness of Mo/Solder A/Die bonding interface under different reflow times. (a) (e) Primary reflow; (b) Secondary reflow; (c) Triple reflow; (d) IMC average thickness after different reflow times.

 DOI:10.30420/566414026

After secondary reflow, the Ni plating layer on MoCu alloy is completely dissolved, and (Ni, Cu)$_3$Sn$_4$ phase is present throughout the entire solder layer. The average thickness of Mo/Solder A and Solder A/Die interfacial IMC layer significantly increases to 3.15 times.

After triple reflow, small voids were found at the interface between MoCu alloy and IMC, which is the Kirkendall effect. During the soldering process, some Cu atoms will diffuse from the MoCu alloy into the solder. It will promote the nucleation of IMC at the interface, allowing IMC to grow in a layered manner. The average thickness of (Ni, Cu)$_3$Sn$_4$ phase at the interface between Mo/Holder A and Solder A/Die is 3.37.

Fig.4 showing interfacial cross section SEM and IMC average thickness of Mo/Solder A/DBC bonding interface under different reflow times. It is resulted that the (Cu, Ni)$_6$Sn$_5$ IMC formed at the welding interface of Mo/Solder A solder joints after primary reflow, and the average thickness of IMC layer is 1.61. After secondary reflow, the average thickness of IMC layer increases to 1.96 times. It is also resulted that the Cu$_6$Sn$_5$ IMC formed at the welding interface of Solder A/DBC solder joints after primary reflow, and the average thickness of IMC layer is 1.61. After secondary reflow, the average thickness of IMC layer increases to 1.66 times.

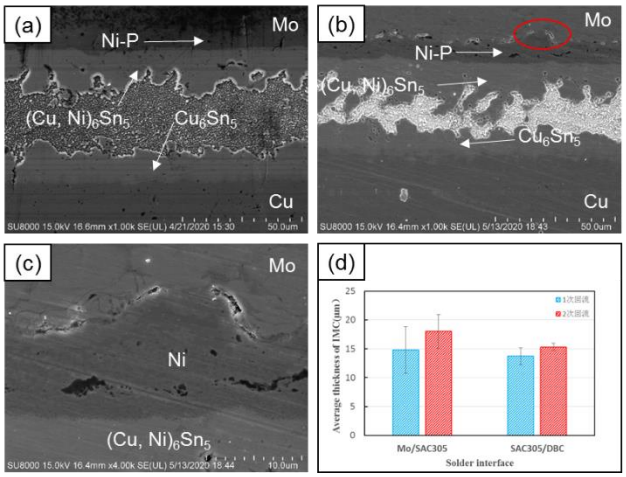

Fig.4. Cross section SEM and IMC average thickness of Mo/Solder A/DBC bonding interface under different reflow times. (a) Primary reflow; (b) (c) Secondary reflow; (d) IMC average thickness after different reflow times.

3.2 Mechanical properties and fracture analysis of the connection interface

Fig.5 showing the shear strength of Mo/Solder A/Die and Mo/Solder A/DBC bonding interface under different reflow times. It is resulted that the shear strength of Mo / Solder A / Die interface increased with the extension of reflowing times before that and decreased a little after that. During primary reflow, the shear strength of the connecting interface was 51.6MPa, which was not significantly different from the shear strength of Solder A, indicating that the fracture was occurred in the solder substrate. After secondary reflow, the shear strength increased to 72.9 MPa, indicating that the fracture crack not only propagates along the solder substrate. After triple reflow, the shear strength decreased to 69.2 MPa, which is related to grain growth and IMC morphology. The shear strength of the Mo/Solder A/DBC connection interface is not significantly different during primary and secondary reflow, which is 70.2 MPa and 74.5 MPa, respectively.

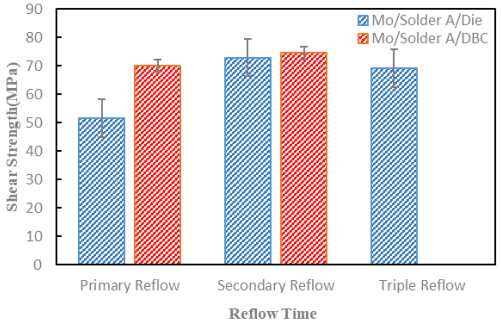

Fig.5. The shear strength of Mo/Solder A/Die and Mo/Solder A/DBC bonding interface under different reflow times.

Fig.6 showing the fracture morphology and fracture mode of Mo/Solder A/Die bonding interface under different reflow times. It can be seen that fracture mainly occurs in solder matrix during primary reflow. A little of (Ni, Cu)$_3$Sn$_4$ phases can be observed on the fracture. Fig.6(d) showing the fracture diagram of bonding interface. After the secondary reflow and triple reflow, the (Ni, Cu)$_3$Sn$_4$ phase increased significantly on the fracture, and the fracture diagram is shown in Fig. 6 (e) and Fig. 6(f).

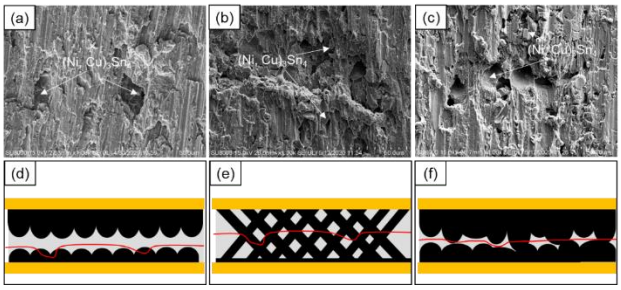

Fig.6. The fracture morphology and fracture mode of Mo/Solder A/Die bonding interface under different reflow times. (a) Primary reflow; (b) Secondary reflow; (c) Triple reflow; (d) the schematic diagram of fracture

mode after primary reflow; (e) the schematic diagram of fracture mode after secondary reflow; (f) the schematic diagram of fracture mode after triple reflow.

Fig.7 showing the fracture morphology and fracture mode of Mo/Solder A/DBC bonding interface under different reflowing times. It can be seen from Fig. 7 (a) that three distinct fracture surfaces can be observed after primary reflow. It is resulted that the fracture position of bonding interface occurs in Cu_6Sn_5 phase, $(Cu, Ni)_6Sn_5$ phase and solder matrix, and the fracture diagram is shown in Fig. 7 (h). Cracks first propagate in the Cu_6Sn_5 phase, then propagate along the substrate solder, and finally propagate along the $(Cu, Ni)_6Sn_5$ phase.

After the secondary reflow, three different fracture surfaces can still be observed. And the fracture diagram is shown in Fig. 7 (i). Cracks also propagate in the Cu_6Sn_5 phase. Due to the increase in IMC thickness after secondary reflow, the intermediate solder matrix is thinner. Subsequently, the crack propagation in the solder matrix is limited, and it will quickly propagate along the $(Cu, Ni)_6Sn_5$ phase. After secondary reflow, the fracture of the connection interface mainly occurs in IMC, so the shear strength of the connection interface is greater than that of the primary reflow.

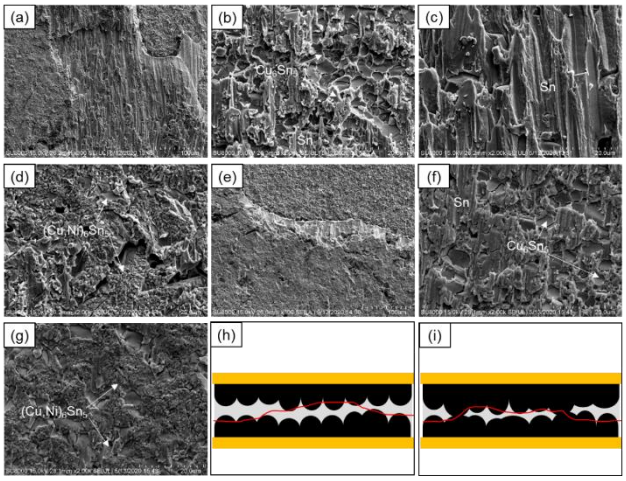

Fig.7. The fracture morphology and fracture mode of Mo/Solder A/DBC bonding interface under different reflow times. (a), (b), (c), (d) Primary reflow; (e), (f), (g) Secondary reflow; (h) the schematic diagram of fracture mode after primary reflow; (i) the schematic diagram of fracture mode after secondary reflow.

4 Conclusion

In this paper, the shear strength and fracture mode of bonding interfaces under different reflow times was also studied. The following conclusions can be drawn:

(1) After reflow soldering, $(Cu, Ni)_6Sn_5$ phase is generated at the interface of Die/Holder A. After reflow soldering, the Solder A/DBC connection interface has η Phase generation. After reflow soldering, $(Cu, Ni)_6Sn_5$ phase is generated at the interface of Mo/Holder A.

(2) The thickness of IMC increases with the increase of reflux times, and the rate of IMC thickness increase decreases with the increase of reflux times.

(3) The shear strength of the Mo/Holder A/Die connection interface increases first and then decreases with the increase of reflux times. As the number of refluxes increases, the fracture of the connection interface changes from ductile fracture occurring in the Sn matrix to a mixed fracture mode occurring at the Sn matrix and IMC.

(4) After a reflow, the Mo/Sander A/DBC connection interface fractures into a mixed fracture mode that occurs in the Cu_6Sn_5 phase, $(Cu, Ni)_6Sn_5$ phase, and Sn matrix, with brittle fracture being the main mode. After secondary reflux, the fracture occurred as brittle fracture in Cu_6Sn_5 and $(Cu, Ni)_6Sn_5$ phases.

5 References

[1] El-Daly AA, Hammad AE. Development of high strength Sn–0.7Cu solders with the addition of small amount of Ag and In. J Alloy Compd 2011; 509:8554–60.

[2] Kotadia HR, Mokhtari O, Clode MP, Green MA, Mannan SH. Intermetallic compound growth suppression at high temperature in SAC solders with Zn addition on Cu and Ni–P substrates. J Alloy Compd 2012; 511:176–88.

[3] Chang SY, Jain CC, Chuang TH, Feng LP, Tsao LC. Effect of addition of TiO2 nanoparticles on the microstructure, microhardness and interfacial reactions of Sn3.5AgXCu solder. Mater Des 2011; 32:4720–7.

[4] A. Wierzbicka-Miernik, K. Miernik, J. Wojewoda-Budka et al., “Microstructure and chemical characterization of the intermetallic phases in Cu/(Sn,Ni) diffusion couples with various Ni additions”, Intermetallics, vol. 59, 2015, 23–31. DOI: 10.1016/j.intermet.2014.12.001.

[5] A.S.M.A. Haseeb, Y.M. Leong, M.M.Arafat, et al., “In-situ alloying of Sn–3.5Ag solder during reflow through Zn nanoparticle addition and its effects on interfacial intermetallic layers”. Intermetallics, vol. 54, 2014, 86–94. DOI: 10.1016/j.intermet.2014.05.011.

[6] L. Liu, Z. Chen, C. Liu, Y. Wu, B. An et al., “Micro-mechanical and fracture characteristics of Cu_6Sn_5 and Cu_3Sn intermetallic compounds under micro-cantilever bending”. Intermetallics, vol. 76, 2016, 10–17. DOI: 10.1016/j.intermet.2016.06.004.

[7] C.H. Wang and H.T. Shen, “Effects of Ni addition on the interfacial reactions between Sn–Cu solders and Ni substrate”. Intermetallics, vol. 18, 2010, 616–622. DOI: 10.1016/j.intermet.2009.10.018.1.15) 368–374.

